

Design and Synthesis of Polymeric Hydrogen Sulfide Donors

Urara Hasegawa^{*,‡,||} and André J. van der Vlies^{†,‡}

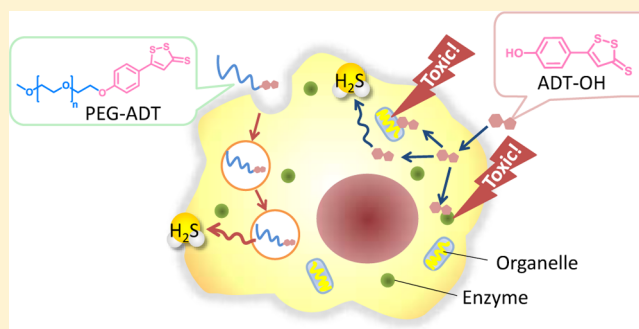
[‡]Department of Applied Chemistry, Graduate School of Engineering, Osaka University, Osaka 565-0871, Japan

^{||}Frontier Research Base for Young Researchers, Graduate School of Engineering, Osaka University, Osaka 565-0871, Japan

[†]Frontier Research Center, Graduate School of Engineering, Osaka University, Osaka 565-0871, Japan

S Supporting Information

ABSTRACT: Hydrogen sulfide (H_2S) is a gaseous signaling molecule that has several important biological functions in the human body. Because of the difficulties of handling H_2S gas, small organic compounds that release H_2S under physiological conditions have been developed. The observed bioactivities of these H_2S donors have generally been directly correlated with their H_2S release properties. However, apart from H_2S release, these H_2S donors also exert biological effects by direct interaction with intracellular components within the cytoplasm after passive diffusion across cellular membranes. Here we report polymeric H_2S donors based on ADT–OH which would alter cellular trafficking of ADT–OH to minimize the unfavorable interactions with intracellular components. We designed and synthesized a poly(ethylene glycol)–ADT (PEG–ADT) conjugate having ADT linked via an ether bond. Whereas ADT–OH significantly reduced cell viability in murine macrophages, the PEG–ADT conjugate did not show obvious cytotoxicity. The PEG–ADT conjugate released H_2S in murine macrophages but not in the presence of serum proteins. The PEG–ADT conjugate was taken up by the cell through the endocytic pathway and stayed inside endolysosomes, which is different from the small amphiphilic donor ADT–OH that can directly enter the cytoplasm. Furthermore, PEG–ADT was capable of potentiating LPS-induced inflammation. This polymeric H_2S donor approach may help to better understand the H_2S bioactivities of the H_2S donor ADT–OH.



INTRODUCTION

Over the past decade, hydrogen sulfide (H_2S) has emerged as the third endogenously produced gaseous transmitter besides nitric oxide (NO) and carbon monoxide (CO).¹ For a long time considered as a toxic compound,^{2,3} currently it has become clear to affect several organ systems and biological processes in the human body.^{4,5} For example, H_2S has been shown to be a regulator of inflammation, promote angiogenesis, modulate blood pressure, and protect cells during ischemia reperfusion and neuro-inflammation. Despite the many publications dealing with H_2S as an important gaseous signaling molecule, it has been recently suggested that persulfides of cysteine and glutathione⁶ or polysulfides ($H_2S_{2,n}$)⁷ are the actual bioactive species. It was proposed that H_2S is generated from cysteine and glutathione persulfides and that H_2S is a marker for their production. This is different from polysulfides that are reported to form by H_2S oxidation.

Along with the understanding of the different roles of H_2S , its therapeutic potential has also been realized.^{8–10} This exogenously delivered H_2S may act directly or indirectly in the form of cysteine and glutathione persulfides or polysulfides because it is well-known that both readily form from H_2S under oxidative conditions.¹¹

To study the biological effects and to solve the difficulty in handling H_2S gas, much research has gone in the development

of donor molecules that can release H_2S under physiological conditions. For delivering H_2S to cells, most studies have used salts like NaHS/ Na_2S that produce H_2S when dissolved in aqueous solutions. Whereas these salts show low cytotoxicity at relatively high dose, the drawbacks in using them as H_2S donors is their uncontrolled release profile. This is especially a problem as it has been suggested that a slow and continuous release is important.^{5,12}

For these reasons, small organic compounds have been reported that can release H_2S under physiological conditions. In general, the observed biological activities of these H_2S donors have been directly correlated with their H_2S release properties. However, what is generally overlooked is that these H_2S donors can directly interact with intracellular biomolecules and organelles, which can affect cellular functions. Therefore, the results obtained with these donor molecules may not be necessary due to H_2S .

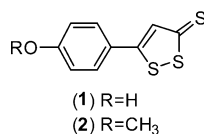
5-(4-Hydroxyphenyl)-3H-1,2-dithiole-3-thione (ADT–OH, Scheme 1), one of the most commonly used H_2S donors, belongs to the class of compounds having the 3H-1,2-dithiole-3-thione group in their structure. Members of this family like 5-

Received: April 6, 2014

Revised: May 26, 2014

Published: June 19, 2014

Scheme 1. Chemical Structures of 5-(4-Hydroxyphenyl)-3H-1,2-dithiole-3-thione (ADT-OH, 1) and 5-(4-Methoxyphenyl)-3H-1,2-dithiole-3-thione (ADT-OCH₃, 2)



(4-methoxyphenyl)-3H-1,2-dithiole-3-thione (ADT-OCH₃) and Oltipraz have been shown to have anticancer properties by activating phase II enzymes.^{13,14} ADT-OCH₃ is a choleric drug marketed as Sulfarlem¹⁵ that has been investigated in chemoprevention in human lung cancer¹⁶ and colon cancer¹⁷ and in rat cancer.¹⁸ This drug also has antioxidative properties by increasing glutathione levels¹⁹ and the hepatoprotective properties due to induction of the phase II detoxification enzymes, in particular NAD(P)H:quinone oxidoreductase and glutathione-S-reductase enzymes.^{20–22} Furthermore, both ADT-OH and ADT-OCH₃ have been shown to inhibit NF-κB activation in human T cells²³ and human estrogen receptor-negative breast cancer via chemical modification.²⁴ This is different from the reported NF-κB activation by H₂S, where sulfhydration is generally believed to cause activation.²⁵

In the field of drug delivery, polymeric therapeutics have been extensively studied.²⁶ In this approach, drugs are conjugated to hydrophilic polymers (polymer–drug conjugates).²⁷ It has been shown that polymeric therapeutics not only improves drug solubility and stability but also prolongs circulation time, reduces side effects, and alters pharmacokinetics and intracellular trafficking.²⁸

In this study, we prepared a polymeric H₂S donor which minimizes the side effects caused by the small donor molecule. We designed and synthesized a poly(ethylene glycol)–ADT (PEG–ADT) conjugate having ADT linked via an ether bond. The cellular toxicity of the PEG–ADT conjugate was compared with ADT-OH and ADT-OCH₃ in murine macrophages. Its H₂S release property was also investigated. Furthermore, the effect on lipopolysaccharide (LPS)-induced inflammation was also evaluated.

RESULTS AND DISCUSSION

Synthesis of PEG–ADT Conjugates Linking ADT via an Ester Bond. Biological activities of ADT-OH in connection with H₂S release has been reported for so-called hybrid molecules in which the ADT-OH moiety is coupled to known drugs like nonsteroidal anti-inflammatory drugs (NSAIDs).^{29,30} The first example of such a compound is ATB-429, linking ADT-OH via an ester bond with mesalamine, which was shown to have reduced toxicity in a murine model of colitis compared to mesalamine alone.^{31,32} Similar reduction of gastrointestinal damaging of NSAIDs were reported for aspirin,³³ diclofenac,³⁴ and naproxen.³⁵ These

effects were ascribed to the anti-inflammatory effect of released H₂S, which was supported by the increase of H₂S plasma levels in rat for mesalamine³⁶ and diclofenac.³⁴ Because these papers used an ester bond to prepare hybrid molecules of ADT-OH and other drugs, we initially prepared the polymer–ADT conjugates using the same approach. To prepare the polymer–ADT conjugate, we used polyethylene glycol (PEG) that has been widely used as a biocompatible polymer in the field of biomaterials. Hydroxyl-terminated methoxy PEG with a nominal molecular weight of 5000 was activated with carbonyldiimidazole and reacted with either glycine (Gly) or isoleucine (Ile) to introduce a carboxylic acid group that was reacted with the phenol group of ADT-OH. Coupling was achieved using dicyclohexylcarbodiimide to afford the PEG–Gly–ADT (7) and PEG–Ile–ADT (8) conjugates (Scheme 2).

Hydrolytic Stability of the PEG–ADT Ester Conjugates. To gain information on the hydrolytic stability of the PEG–Gly–ADT conjugate, we prepared solutions in PBS (pH 7.4) and incubated at 37 °C. At different time points, the mixture was acidified with acetic acid and lyophilized. ¹H NMR of the freeze-dried samples was measured to quantify the extent of hydrolysis by comparing the integral values of the olefinic CH proton of ADT-OH and ADT linked by the ester bond at 7.82 and 7.68 ppm, respectively. As can be seen in Figure 1, the

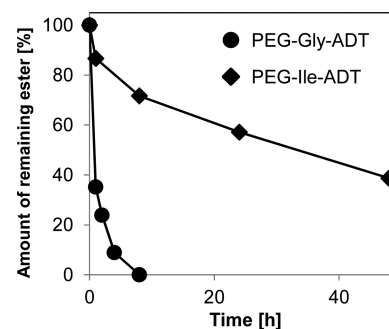
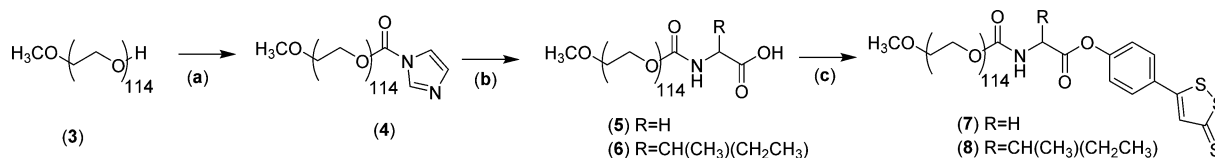


Figure 1. Hydrolysis kinetics of the PEG–Gly–ADT and PEG–Ile–ADT conjugates in PBS (pH 7.4) at 37 °C as measured by ¹H NMR.

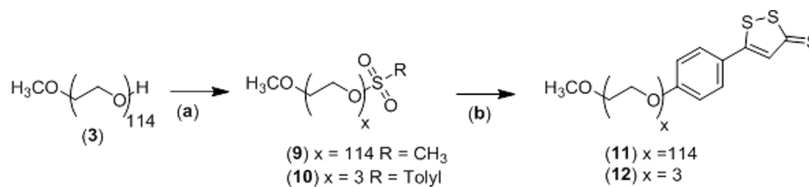
PEG–Gly–ADT conjugate hydrolyzed quickly with an estimated half-life of about 30 min. This hydrolysis was also macroscopically visible by the occurrence of an orange precipitate due to the poor solubility of ADT-OH in PBS. With such a fast chemical hydrolysis rate, the conjugate is also expected to be cleaved in serum due to the presence of esterase.

Indeed, the UV/vis spectrum of the PEG–Gly–ADT conjugate in 10% fetal bovine serum (FBS) after 2 h shows spectral changes due to the partial hydrolysis of the conjugate (Supporting Information Figure S1). Because hydrolysis of the PEG–Gly–ADT conjugate would be too fast for our application, we investigated whether we could slow down hydrolysis by changing the chemical environment around the

Scheme 2. Preparation of the PEG–Gly–ADT and PEG–Ile–ADT Conjugates Having ADT Linked via an Ester Bond^a



^a(a) CDI, DMSO, (b) glycine or isoleucine, Et₃N, DMSO, 80 °C, (c) ADT-OH, DCC, DMAP, CH₂Cl₂.

Scheme 3. Preparation of the PEG–ADT Conjugate and TEG–ADT Having ADT Linked via an Ether Bond^a

^a(a) Methanesulfonyl chloride, Et₃N, toluene; (b) ADT–OH, K₂CO₃, DMF, 80 °C.

ester. We therefore tested the hydrolysis of the PEG–Ile–ADT conjugate with the idea that the bulky and hydrophobic *sec*-butyl group would avoid ester hydrolysis. Although much slower, hydrolysis still occurred and about 50% was hydrolyzed after 30 h as shown in Figure 1.

Synthesis PEG–ADT Conjugate Linking ADT via an Ether Bond. In our concept of a polymeric ADT-based H₂S donor, the ester conjugates were not suited due to rapid ester hydrolysis. We therefore focused our attention on the preparation of a PEG conjugate linking ADT via a noncleavable ether bond as shown in Scheme 3. Nucleophilic substitution of ADT–OH with PEG mesylate afforded the PEG–ADT (11) conjugate. To confirm the structure of the PEG–ADT conjugate, we also prepared a small molecule linking ADT to three ethylene glycol units (TEG–ADT, 12) and characterized this compound by ¹H NMR and high resolution mass spectrometry. The chemical shifts of the signals due to the ADT moiety of this model compound were identical with that of the PEG–ADT conjugate confirming its structure.

Cellular Toxicity of the PEG–Gly–ADT, PEG–Ile–ADT, and PEG–ADT Conjugates. ADT–OH is known to reduce cell viability by inhibiting histone deacetylase^{37,38} and NF-κB activation.²³ Here we tested the effect of PEG conjugation on the cytotoxicity of ADT–OH. As shown in Figure 2, ADT–

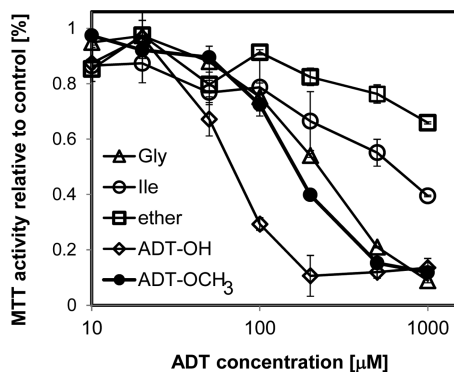


Figure 2. Cell viability of RAW-Blue cells treated with PEG–Gly–ADT, PEG–Ile–ADT, and PEG–ADT. ADT–OCHH₃, and ADT–OH for 24 h (MTT assay).

OH significantly reduced metabolic activity in RAW-Blue macrophages as measured by the MTT assay. The live/dead assay showed that the majority of cells apoptosed and detached from the glass surface (Figure 3). On the other hand, conjugation of ADT–OH to PEG reduced cellular toxicity (Figure 2). This reduced toxicity is not due to alkylation of the phenol group as shown by the toxicity profile of ADT–OCH₃ (Figure 2). The hydrolysis rate of the PEG–Gly–ADT and PEG–Ile–ADT conjugates significantly affects toxicity in the cells. The MTT assay showed that the PEG–Gly–ADT

conjugate with an unstable linkage was more toxic than the PEG–Ile–ADT conjugate which showed much slower release of ADT–OH. A similar trend was observed in the live/dead assay as shown in Figure 3. For the nonhydrolyzable PEG–ADT conjugate, no obvious cellular toxicity was observed in the live/dead assay unlike the PEG–Gly–ADT and PEG–Ile–ADT conjugates (Figure 3). On the other hand, a slight reduction in metabolic activity was observed at concentrations above 200 μM in the MTT assay (Figure 2).

To confirm that ADT–OH released from the conjugates exerted the toxicity in the cells, the UV/vis spectrum of the culture medium containing the PEG–Gly–ADT and PEG–ADT conjugates was measured after incubation with RAW-Blue macrophages (Supporting Information Figure S1). The typical UV/vis spectrum of ADT–OH (Supporting Information Figure S1) was observed for the PEG–Gly–ADT conjugate, while the spectrum of ADT–OH was not observed in the case of the PEG–ADT conjugate, indicating that hydrolysis did not occur. To show chemical evidence for the release of ADT–OH in culture, cells with medium that had been incubated with PEG–Gly–ADT and PEG–Ile–ADT were lyophilized. After extraction and aqueous workup, ¹H NMR showed the presence of ADT–OH (Supporting Information Figure S2). Therefore, the cellular toxicities of the PEG–Gly–ADT and PEG–Ile–ADT conjugates were due to released ADT–OH after hydrolysis.

It is interesting to note that most studies using ADT–OH linked with another molecule via an ester bond do not mention this hydrolysis. Our data of the PEG–Gly–ADT and PEG–Ile–ADT conjugates suggests that this is a point to consider in evaluating the bioactivity of such compounds.

H₂S Release from the PEG–ADT Conjugate. Contrary to other H₂S donors allyldisulfide/allyltrisulfide,³⁹ thiobenzenamides,⁴⁰ and GYY 4137,¹² the precise mechanism for H₂S release from ADT–OH is not clear. A direct hydrolysis mechanism, in which the thiocarbonyl is converted to a carbonyl group with concomitant H₂S release, has been suggested.⁴¹ However, such a mechanism seems unlikely because a derivative of ADT–OH was only completely hydrolyzed after 48 h in PBS/DMSO at 120 °C. It is therefore more likely that an enzymatic step is involved. It has been reported that ADT–OH released H₂S in rat liver homogenate and rat plasma but significantly less in buffer alone.³⁴ In addition, it has been also reported that isolated mitochondria from U373 cells were able to induce H₂S release, suggesting that reductive enzymes as present in mitochondria are responsible.⁴² To see whether the PEG–ADT conjugate was capable of releasing H₂S, we used a H₂S-specific electrode to monitor H₂S release. Because ADT–OH and ADT–OCH₃ contains a disulfide linkage that can be reduced electrochemically,⁴³ we investigated if a simple chemical, i.e., nonenzymatic, reduction could induce H₂S release. We first used the reducing

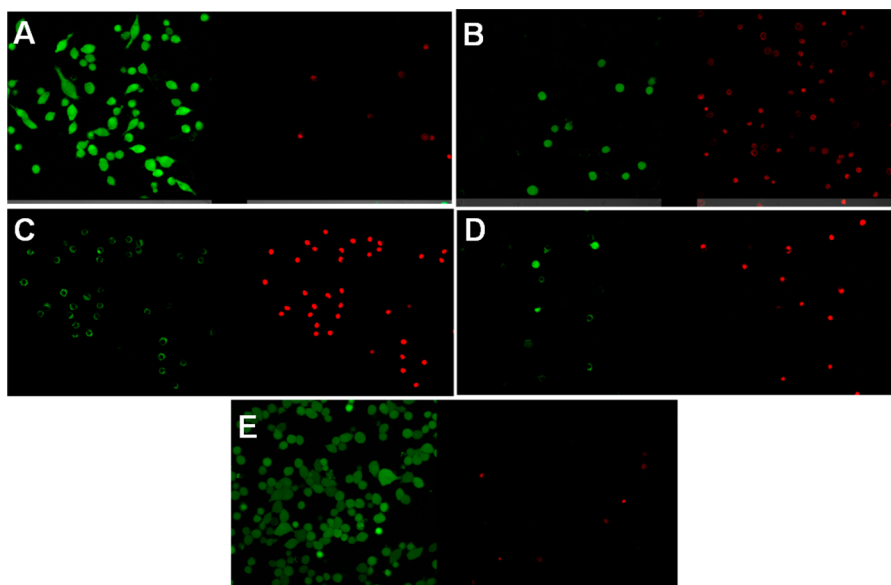


Figure 3. CLSM images showing live (green) and dead (red) RAW-Blue macrophages after incubating for 24 h with (A) PEG-ADT, (B) PEG-Ile-ADT, (C) PEG-Gly-ADT, (D) ADT-OH, and (E) control (without treatment). Concentration of PEG-ADT, PEG-Ile-ADT, PEG-Gly-ADT, and ADT-OH: 200 μM .

agents such as coenzyme NADH, L-cysteine, and glutathione, which are present within the cell. Treating the PEG-ADT conjugate with these compounds at pH 7.4 did not induce H_2S release (data not shown), showing its stability against reduction but also hydrolysis. Other reducing agents such as hydrazine and dithiothreitol were also not able to induce H_2S release (data not shown). Only when TCEP, a water-soluble phosphine reducing agent, was used, H_2S release was detected (Figure 4). Running the experiment on a larger scale, the

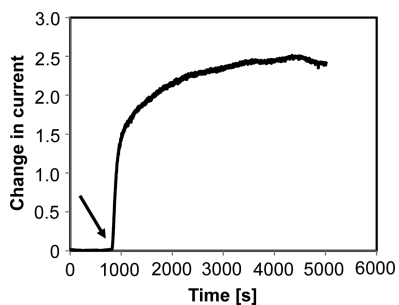


Figure 4. H_2S release from the PEG-ADT conjugate (20 μM) in the presence of TCEP-HCl (500 μM) in PBS (pH7.4) as measured by the change in the current using a H_2S electrode sensor. The arrow indicates the addition of TCEP.

release of H_2S was also indicated qualitatively by the typical smell of H_2S and the formation of brown lead sulfide (PbS) after exposing the head space to filter paper impregnated with lead acetate (Supporting Information Figure S3). ADT-OH and ADT-OCH₃ also released H_2S in response to TCEP as confirmed by the formation of PbS (Supporting Information Figure S3). Because TCEP readily reduces disulfide bonds within proteins, it is likely that the first step is reduction of the -S-S- of the trithione followed up by another reaction that finally releases H_2S . Because L-cysteine and glutathione are not able to induce H_2S release from the PEG-ADT conjugate, it seems unlikely that a simple chemical reduction can induce H_2S release in the body.

To see whether serum proteins could induce H_2S release, we incubated the PEG-ADT conjugate, ADT-OH, and ADT-OCH₃ in 10% fetal bovine serum (FBS). Because it was reported that ADT-OH releases H_2S in the presence of FBS,⁴⁴ we expected that the PEG-ADT conjugate would release H_2S . Contrary to our expectation, no H_2S release was observed for the PEG-ADT conjugate and ADT-OCH₃ in 10% FBS (Figure 5).

Only for ADT-OH, H_2S release was observed as shown in Supporting Information Figure S4. In addition, a rapid H_2S release was also measured when the experiment was repeated in PBS. Strangely, we noticed that the signal was increasing continuously and that it took a long time to equilibrate the electrode after removing the reaction mixture. We therefore suspected that the increase of the signal was caused by the interaction of ADT-OH with the electrode. To confirm this, we used lead acetate to detect released H_2S from a solution of ADT-OH as described for the PEG-ADT conjugate. After 1 week, only the ADT-OH solution containing TCEP showed a black color due to the formation of PbS while no obvious color change was observed for ADT-OH in PBS (Supporting Information Figure S5). This suggests that H_2S release from ADT-OH in PBS is not significant or absent. On the basis of these observations, we believe that the H_2S release profile of ADT-OH in PBS and 10% FBS is an artifact.

We next investigated whether intracellular enzymes could induce H_2S release. The PEG-ADT conjugate and ADT-OCH₃ were added to cell lysate from RAW-Blue macrophages and H_2S release was measured by the H_2S electrode sensor. As can be seen from Figure 5A, the PEG-ADT conjugate released H_2S in the presence of cell lysate. ADT-OCH₃ also showed H_2S release, and the amount of released H_2S was 10 times higher than that of the PEG-ADT conjugate as shown in Figure 5B. To show that the H_2S release profiles for ADT-OCH₃ and PEG-ADT were not due to an artifact as was observed for ADT-OH, two additional experiments were done. We used the fluorescent H_2S detection dye, WSP-1 (Supporting Information Scheme S1)⁴⁵ and measured the

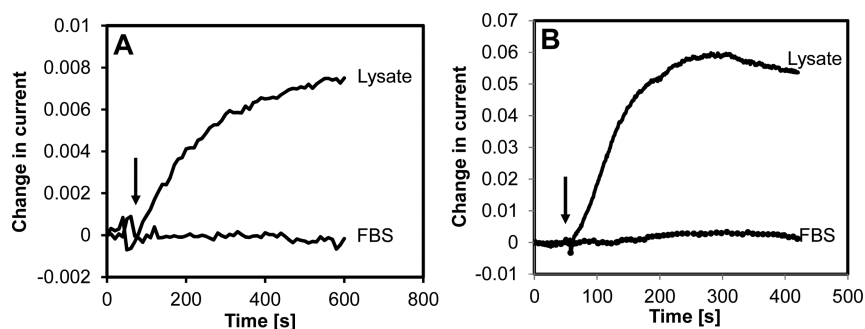


Figure 5. H₂S release from (A) the PEG-ADT conjugate and (B) ADT-OCH₃ (50 μM) in 10% FBS and cell lysate as measured by the change in the current using a H₂S electrode sensor. The arrow indicate when PEG-ADT and ADT-OCH₃ were added.

increase in fluorescence of ADT-OCH₃ and PEG-ADT solutions in cell lysate. For both ADT-OCH₃ and PEG-ADT, a higher fluorescence was measured compared to cell lysate alone (Supporting Information Figure S6). The fluorescence experiments showed a similar trend in which ADT-OCH₃ showed higher release. Furthermore, we also detected H₂S in the gas phase using a similar setup as that used in the PbS experiments (Supporting Information Figure S7). To increase sensitivity, we used dansylazide instead of Pb(OAc)₂ to detect H₂S. Dansylazide forms a fluorescent product with H₂S and has been used to quantify H₂S in blood samples.⁴⁶ As shown in Supporting Information Figure S7, both ADT-OCH₃ and PEG-ADT showed higher H₂S release compared to cell lysate alone. These results suggest that an intracellular component(s), presumably an enzyme, induces H₂S release. In the case of PEG-ADT, the ADT moiety is sterically hindered by PEG from interacting with proteins, which may reduce the amount of H₂S released. Furthermore, it should be noted that the experiments were not carried out under strict anaerobic conditions. Thus, released H₂S would be partially oxidized in this experiment. It can be expected that oxidation of H₂S might become a significant competing reaction when the rate of H₂S generation is slow. Thus, the lower amount of H₂S release from the PEG-ADT conjugate is partially attributed to the slower H₂S generation for the PEG-ADT conjugate compared to ADT-OCH₃.

To observe H₂S release under more relevant conditions, we incubated the PEG-ADT conjugate with RAW-Blue macrophages. To determine the H₂S concentration in the culture medium, we used WSP-1. As can be seen in Figure 6, the H₂S concentration gradually increased up for 1 h upon the addition

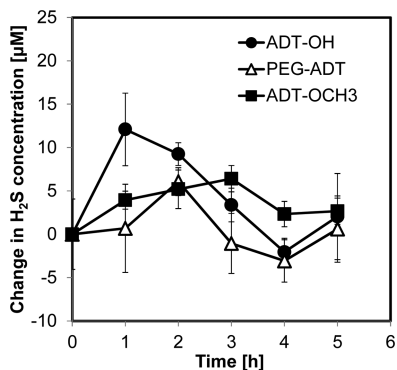


Figure 6. H₂S release from ADT-OH, ADT-OCH₃, and the PEG-ADT conjugate in the presence of RAW-Blue macrophages. Concentration: 100 μM.

of ADT-OH. In case of ADT-OCH₃, the H₂S concentration steadily increased for the first 3 h and then declined. For the PEG-ADT conjugate, the increase of H₂S concentration was much lower compared to the small H₂S donors, which is consistent with the H₂S release profile in the presence of cell lysate (Figure 5).

Intracellular Distribution of the PEG-ADT Conjugate.

To see the intracellular distribution of H₂S donors in RAW-Blue macrophages, we prepared FITC-labeled ADT-OH and PEG-ADT conjugate (for details, see Schemes S2 and S3 in the Supporting Information). To visualize the endolysosomes, Rhodamine-labeled dextran was used as a marker. While ADT-OH was present homogeneously in the cytoplasm, the PEG-ADT conjugate colocalized with the endolysosomes that appeared as yellow spots in the merged images (Figure 7). It is well-documented that amphiphilic small molecules can diffuse across cellular membranes and directly enter the cytoplasm.⁴⁷ In contrast, macromolecules which normally cannot pass through the lipid bilayer enter cells by endocytosis and remain inside the endolysosome compartment.⁴⁸ Therefore, the different distribution between ADT-OH and the PEG-ADT conjugate can be attributed to these size effects on the cellular uptake behavior.

This altered intracellular distribution of the PEG-ADT conjugate seems to correlate with the reduced toxicity relative to ADT-OH. It has been reported that besides being a H₂S donor, ADT-OH as well as other trithione derivatives can directly interact with intracellular enzymes and organelles and exert biological activities including antiproliferative, chemopreventive, and anticarcinogenic properties.^{16–18,49} As these interactions with intracellular components occur in the cytoplasm, it can be expected that the side effects of ADT-OH could be minimized by preventing its passive diffusion through the cellular membranes to enter the cytoplasm. As shown in Figure 7B, the PEG-ADT conjugate stayed inside the endolysosomes without escaping to other cellular compartments. Therefore, together with the cytotoxicity data, the trapping of the ADT structure in the endolysosomes by the PEG-ADT conjugate seems to be a key to prevent unfavorable side effects of ADT-OH.

Furthermore, the intracellular distribution of these polymeric formulations also offers insight into the H₂S release mechanism. As shown in Figure 5, it is suggested that the H₂S release was induced by intracellular enzymes. Also, we showed that the PEG-ADT conjugate was capable of releasing H₂S in the presence of RAW-Blue macrophages as shown in Figure 6. These observations together with the intracellular distribution data indicate that enzymes locating inside the endolysosomes

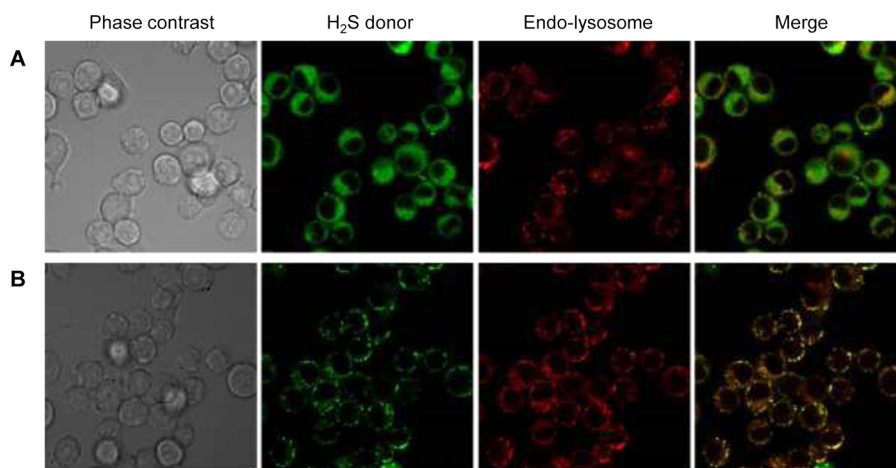


Figure 7. Intracellular distribution of fluorescently labeled ADT-OH (A) and the PEG-ADT conjugate (B) in RAW-Blue macrophages. Concentration: 70 μM for ADT-OH, 100 μM for the PEG-ADT conjugate.

are probably responsible for H_2S release from the PEG-ADT conjugate although further investigation is necessary to elucidate the exact mechanism.

Effect of the PEG-ADT Conjugate on LPS-Induced Inflammation. Several studies suggested that endogenously produced H_2S enhance pro-inflammatory responses in acute inflammation such as sepsis although the role of H_2S in inflammation is complex, with both pro- and anti-inflammatory effects reported.³⁰ We investigated the effect of the PEG-ADT conjugate in lipopolysaccharide (LPS)-induced inflammation. LPS is a ligand for Toll-like receptor 4 (TLR4) found on immune cells that initiate an immunological reaction upon bacterial infection. RAW-Blue macrophages were stimulated with LPS in the presence of the PEG-ADT conjugate, ADT-OH, and Na_2S , a sulfide salt known as an rapid H_2S releaser. The production of the pro-inflammatory cytokine tumor necrosis factor ($\text{TNF-}\alpha$) was quantified after 2 h as shown in Figure 8.

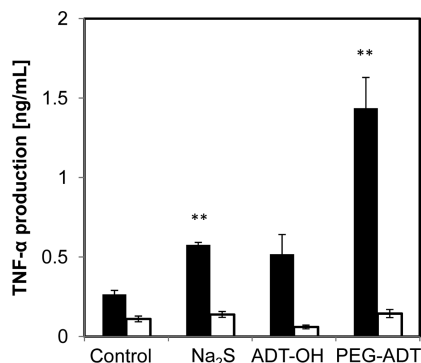


Figure 8. Effect of the different H_2S donors (50 μM) on $\text{TNF-}\alpha$ production upon lipopolysaccharide (LPS) stimulation. Solid column, LPS (+); empty column, LPS (-). ** $p < 0.01$ versus control, LPS (+).

Upon the addition of Na_2S and the PEG-ADT conjugate, the $\text{TNF-}\alpha$ production was significantly enhanced in RAW-Blue macrophages stimulated with LPS, whereas the H_2S donors by themselves (without LPS stimulation) did not increase $\text{TNF-}\alpha$ levels compared to the control. In addition, a much higher $\text{TNF-}\alpha$ level was observed for the PEG-ADT conjugate

compared to Na_2S . This result may be due to the different H_2S release profiles of these donors. Furthermore, ADT-OH also seems to promote inflammation upon LPS stimulation, although its effect was not statistically significant. Because ADT-OH is known to inhibit the transcriptional factor NF- κB which plays a key role in immunological response to pathogens,²³ the reduced activity may be caused by the biological effect of ADT-OH itself.

CONCLUSION

We have designed and synthesized polymeric H_2S donors based on the small H_2S donor ADT-OH. The PEG-Gly-ADT and PEG-Ile-ADT conjugates readily hydrolyzed and released ADT-OH, resulting in reduced cellular viability as shown by the MTT and live/dead assay. On the other hand, the PEG-ADT conjugate having a noncleavable ether bond did not show obvious cellular toxicity. This reduced toxicity seems to correlate with the colocalization of the PEG-ADT conjugate with the endolysosomes without escaping to the cytoplasm. The PEG-ADT conjugate was capable of releasing H_2S in the presence of murine macrophages. Furthermore, PEG-ADT was capable of potentiating LPS-induced inflammation. The PEG-ADT conjugate may provide a tool that can give complementary information for a better understanding of the H_2S donor ADT-OH within cells.

EXPERIMENTAL PROCEDURES

Materials. Methoxy-polyethylene glycol with a nominal molecular weight of 5000 (mPEG₁₁₄OH), isoleucine (Ile), NADH, L-cysteine, (reduced) glutathione, hydrazine, TCEP-HCl, and (2-(2-(2-methoxyethoxy)ethoxy)ethoxy)*p*-toluenesulfonate were from Sigma-Aldrich. Carbonyldiimidazole (CDI), dimethyl sulfoxide (DMSO), triethylamine (Et₃N), glycine (Gly), sodium hydrogensulfate hydrate ($\text{NaHSO}_4 \cdot \text{H}_2\text{O}$), anhydrous sodium sulfate (Na_2SO_4), anhydrous potassium carbonate (K_2CO_3), dicyclohexylcarbodiimide (DCC), ninhydrin, potassium hydroxide (KOH), diethyl ether (Et₂O), and anhydrous dimethylformamide (DMF) were from Wako Pure Chemical Industry. 4-Dimethylaminopyridine (DMAP) and thiazolyl Blue tetrazolium bromide (MTT) were from Tokyo Chemical industry (TCI). Dichloromethane (CH_2Cl_2), chloroform (CHCl_3), ethyl acetate (EtOAc), and molecular sieves 3A were from Nacalai Tesque. LPS-free water was purchased from

Otsuka Pharmaceutical Factory. DMEM GlutaMax, fetal bovine serum (FBS), penicillin–streptomycin, and live/dead cell viability assay kit were purchased from Invitrogen. Lipopolysaccharide (LPS) was purchased from Invivogen. Passive lysis buffer was purchased from Promega. WSP-1 was purchased from Cayman Chemical. RAW-Blue macrophages, QUANTI-Blue, and Zeocin were purchased from Invivogen. Triple-well glass-based dishes and 96-well microplates were purchased from Iwaki. Water was freed from salt using the Milli-Q water system.

Synthesis. All reactions were done in an inert argon atmosphere, and chemicals were used as received unless stated otherwise. Molecular sieves were dried at 180 °C under reduced pressure. Et₃N was distilled from ninhydrin and KOH and stored over molecular sieves. CH₂Cl₂ was dried over molecular sieves.

ADT–OH (1). ADT–OH (1) was prepared as reported.³⁴

mPEG₁₁₄–CDI (4). First, 10.9 g (2.2 mmol) of mPEG₁₁₄–OH (3) was heated at 80 °C under reduced pressure to remove water. After cooling down to RT, the solid was dissolved in 40 mL of DMSO and 1.68 g (10.4 mmol, 4.8 equiv) of CDI was added to the clear solution. After stirring for 24 h, the solution was diluted with 500 mL of EtOAc and put at –20 °C. After 2 h, a white solid precipitated that was filtered and washed with Et₂O (2 × 100 mL). After drying under reduced pressure, this yielded 10.2 g (94%) of a white solid. ¹H NMR (DMSO-*d*₆) δ = 8.25 (s, 1H, CH_{imidazole}), 7.59 (s, 1H, CH_{imidazole}), 7.08 (s, 1H, CH_{imidazole}), 4.50 (m, 2H, CH₂–CO–N), 3.76–3.35 (m, CH₂CH₂O), and 3.24 (s, 3H, OCH₃). The degree of functionalization, calculated from the integral values of the imidazole and the methoxy signals, was 100%.

mPEG₁₁₄–Gly (5). First, 1.0 g (0.21 mmol) (4) was dissolved in 5 mL of DMSO and to the clear solution was added 75.9 mg (1.0 mmol, 4.9 equiv) of glycine followed by 141 μL (1.0 mmol, 4.9 equiv) of Et₃N and the mixture was heated at 80 °C. After 29 h, the yellow mixture was diluted with 25 mL of 1 M NaHSO₄ (aq) and extracted with CH₂Cl₂ (3 × 25 mL). After drying over Na₂SO₄, the solution was concentrated to a small volume, diluted with 200 mL of EtOAc, and kept at –20 °C for 2 h. The precipitate was filtered, washed with EtOAc (25 mL) and Et₂O (100 mL) and dried under reduced pressure to yield 897 mg (87%) of a white solid. ¹H NMR (DMSO-*d*₆) δ = 12.5 (bs, 1H, CO₂H), 7.41 (bs, 1H, NH), 4.05 (m, 2H, CH₂–C(O)), 3.76–3.35 (m, CH₂CH₂O + NH–CH₂–CO₂H), 3.24 (s, 3H, OCH₃). The degree of functionalization, calculated from the integral values of the CH₂–C(O) and methoxy signals, was 91%.

mPEG₁₁₄–Ile (6). First, 1.0 g (0.21 mmol) (4) was dissolved in 10 mL of DMSO, and then to the clear solution was added 262 mg (2.0 mmol, 9.5 equiv) of isoleucine followed by 279 μL (2.1 mmol, 10 equiv) of Et₃N and the mixture heated at 80 °C. After 23 h, the yellow mixture was diluted with 25 mL of 1 M NaHSO₄ (aq) and extracted with CH₂Cl₂ (3 × 25 mL). After drying over Na₂SO₄, the clear solution was concentrated under reduced pressure to give a liquid that was diluted with 200 mL of EtOAc and placed at –20 °C for 3 h. The precipitate was filtered and washed with 200 mL of Et₂O and dried under reduced pressure and yielded 925 mg (88%). ¹H NMR (DMSO-*d*₆) δ = 12.5 (bs, 1H, CO₂H), 7.43 (bs, 1H, NH), 4.05 (m, 2H, CH₂–C(O)), 3.85 (m, 1H, NH–CH–CO₂H), 3.76–3.53 (m, CH₂CH₂O), 3.24 (s, 3H, OCH₃), 1.76 (m, 1H, CHCH₃), 1.38 (m, 1H, CH–CH₂–CH₃), 1.24 (m, 1H, CH–CH₂–CH₃), 0.84 (m, 6H, 2 × CH₃). The degree of functionalization,

calculated from the integral values of the methyl and methoxy signal, was 93%.

PEG–Gly–ADT (7). First, 513 mg (0.1 mmol) of (5) and 24.6 mg (0.11 mmol, 1.1 equiv) of (1) were dissolved in 10 mL of CH₂Cl₂. To the solution was added 22.9 mg (0.11 mmol, 0.11 equiv) of DCC in 1 mL of CH₂Cl₂ followed by 1.3 mg (0.011 mmol, 0.11 equiv) of DMAP in 109 μL of CH₂Cl₂. The mixture was stirred for 28 h and concentrated under reduced pressure. The residue was suspended in 25 mL of 1 M NaHSO₄ (aq) and filtered to remove DCU. The aqueous phase was extracted with CH₂Cl₂ (3 × 25 mL) and after combining dried over Na₂SO₄. The clear solution was concentrated to about 10 mL and diluted with Et₂O (400 mL). The orange precipitate was filtered, washed with Et₂O (100 mL), and dried under reduced pressure to yield 414 mg (81%) of an orange solid. ¹H NMR (DMSO-*d*₆) δ = 7.99 (d, 2H, 2 × CH_{aromat} ADT), 7.85 (bs, 1H, NH), 7.83 (s, 1H, CH=C ADT), 7.31 (d, 2H, 2 × CH_{aromat} ADT), 4.11 (s, 2H, NH–CH₂–C(O)), 4.08 (m, 2H, CH₂–C(O)–NH), 3.76–3.53 (m, CH₂CH₂O), 3.24 (s, 3H, OCH₃). The degree of functionalization, calculated from the integral values of the ADT and methoxy signals, was 95%.

PEG–Ile–ADT (8). First, 507 mg (0.1 mmol) of (6) and 33.1 mg (0.15 mmol, 0.15 equiv) of (1) were dissolved in 10 mL of CH₂Cl₂ and 1.8 mg (0.015 mmol, 0.15 equiv) of DMAP in 375 μL of CH₂Cl₂ and 33.7 mg (0.16 mmol, 0.16 equiv) of DCC in 1 mL of CH₂Cl₂ were added. After stirring, the mixture for 19 h, the solution was concentrated and the residue suspended in 25 mL of 1 M NaHSO₄ (aq). After filtering, the clear solution was extracted with CH₂Cl₂ (3 × 25 mL), dried over Na₂SO₄ concentrated to a small volume, and diluted with 400 mL Et₂O. The solid was collected, washed with 100 mL of Et₂O, and dried under reduced pressure to yield 486 mg (96%) of orange solid. ¹H NMR (DMSO-*d*₆) δ = 7.99 (d, 3H, 2 × CH_{aromat} ADT + NH), 7.83 (s, 1H, CH=C ADT), 7.31 (d, 2H, 2 × CH_{aromat} ADT), 4.19 (m, 1H, NH–CH–C(O)O), 4.12 (m, 2H, CH₂–C(O)–NH), 3.76–3.35 (m, CH₂CH₂O), 3.24 (s, 3H, OCH₃), 1.95 (m, 1H, CHCH₃), 1.70 (m, 1H, CH–CH₂–CH₃), 1.52 (m, 1H, CH–CH₂–CH₃), 0.98 (d, 3H, CHCH₃), 0.89 (t, 3H, CH₂–CH₃). The degree of functionalization, calculated from the integral values of ADT and the methoxy signals, was 63%.

mPEG₁₁₄–Mesylate (9). 9 was prepared according to that reported.⁵⁰ First, 21.0 g (4.2 mmol) of (3) was dissolved in 600 mL of toluene and dried by azeotropic distillation using a Dean–Stark trap. After 80 mL of toluene/H₂O was collected, the mixture was cooled to 30 °C. To the clear solution was added 1.6 mL (21 mmol, 5 equiv) of methanesulfonyl chloride and 2.9 mL (21 mmol, 5 equiv) of Et₃N. The mixture became hazy within 1 min. After 19 h, the mixture was filtered through SiO₂ (2.5 cm diameter × 2.0 cm height) and concentrated under reduced pressure. The oily residue was dissolved in 25 mL of CH₂Cl₂ and added to 1 L of Et₂O. The white precipitate was collected, washed with Et₂O (2 × 100 mL), and dried under reduced pressure to yield 19.5 g (3.9 mmol, 92%). ¹H NMR (CDCl₃): δ = 4.36 (m, 2H, CH₂OSO₂), 3.81–3.43 (m, CH₂CH₂O PEG), 3.36 (s, 3H, OCH₃ PEG), 3.07 (s, 3H, SO₂CH₃). The degree of functionalization, calculated from the integral values of the mesylate and the methoxy signals, was 100%.

PEG–ADT (11). First, 1.0 g (0.2 mmol) of (9), 91 mg (0.4 mmol, 2 equiv) of (1), and 54 mg (0.4 mmol, 2 equiv) of K₂CO₃ were dissolved in 10 mL of DMF and heated at 80 °C for 24 h. The mixture was then cooled to RT and concentrated under reduced pressure. The residue was partitioned in 50 mL

of CH_2Cl_2 and 50 mL of 1 M NaHSO_4 (aq). After separating both layers, the aqueous phase was extracted with CH_2Cl_2 (2×50 mL) and the combined extracts were dried over Na_2SO_4 and concentrated under reduced pressure to 20 mL. The solution was then added to 300 mL of Et_2O , and the orange solid was collected. After washing with Et_2O (4×50 mL), the solid was dried under reduced pressure, yielding 817 mg (0.16 mmol, 82%). $^1\text{H NMR}$ (CDCl_3): $\delta = 7.60$ (d, 2H, $2 \times \text{CH}_{\text{aromat}}$ ADT), 7.38 (s, 1H, $\text{CH}=\text{C}$ ADT), 6.99 (d, 2H, $2 \times \text{CH}_{\text{aromat}}$ ADT), 4.18 (t, 2H, CH_2OPh), 3.88–3.47 (m, $\text{CH}_2\text{CH}_2\text{O}$ PEG), 3.37 (s, 3H, OCH_3 PEG). The degree of functionalization, calculated from the integral values of the ADT and methoxy signals, was 89%.

(2-(2-(2-Methoxyethoxy)ethoxy)ethoxy)–ADT (TEG–ADT, 12). First, 129 mg (0.41 mmol) (2-(2-(2-methoxyethoxy)ethoxy)ethoxy)*p*-toluenesulfonate, 102 mg (0.45 mmol) (1), and 63 mg (0.45 mmol) K_2CO_3 were dissolved in 5 mL of DMF and heated at 80 °C for 18 h. After cooling down to RT, the mixture was then concentrated and 50 mL of CHCl_3 added. The suspension was filtered, and the residue was washed with CHCl_3 (2×50 mL). The filtrate was concentrated and the residue purified by SiO_2 column chromatography ($R_f = 0.46$, EtOAc /hexane 4:1). This yielded 125 mg (0.34 mmol, 82%) of a red oil. $^1\text{H NMR}$ (CDCl_3): $\delta = 7.60$ (d, 2H, $2 \times \text{CH}_{\text{aromat}}$ ADT), 7.39 (s, 1H, $\text{CH}=\text{C}$ ADT), 6.99 (d, 2H, $2 \times \text{CH}_{\text{aromat}}$ ADT), 4.19 (t, 2H, CH_2O), 3.88 (t, 2H, CH_2), 3.74 (t, 2H, CH_2), 3.68 (t, 2H, CH_2), 3.65 (m, 2H, CH_2), 3.50 (t, 2H, CH_2), 3.38 (s, 3H, OCH_3). MS (*m/z*, $\text{M} + \text{Na}^+$, ESI-TOF-MS): calculated for $\text{C}_{16}\text{H}_{19}\text{O}_3\text{S}_3$ 395.0415, found 395.0406.

Dansylazide. Dansylazide was prepared as reported.⁴⁶

Time Course Hydrolysis Experiment. Stock solutions of PEG–Gly–ADT and PEG–Ile–ADT at 420 μM were prepared in 10 mM PBS (pH 7.4). The stock solutions were then split into several 15 mL of Falcon tubes and put at 37 °C in a bioshaker. At different time points, a tube was taken out, acidified with acetic acid 1% (v/v), frozen, and stored at –20 °C. After the last sample was collected, all samples were lyophilized. To each tube was then added 800 μL of $\text{DMSO}-d_6$ and put on a sample rotator for 6 h. After spinning down insoluble salts, the clear supernatant was measured by $^1\text{H NMR}$ to determine the extent of hydrolysis.

Extraction of ADT–OH from Cell Cultures. RAW-Blue were seeded at 100000 cells/well with 200 μL of medium and cultured overnight. The supernatant was replaced with 200 μL of medium containing PEG–Gly–ADT and PEG–Ile–ADT at 1 mM. The cells were cultured for 24 h, after which the well plate was frozen and lyophilized. For each conjugate, three wells were extracted with 3 mL of MeOH. The yellow mixture was concentrated under reduced pressure, and the orange residue acidified with 5 mL of 1 M NaHSO_4 (aq) and extracted with CH_2Cl_2 (3×5 mL). After drying over Na_2SO_4 , the yellow solution was concentrated under reduced pressure. The residue was dissolved in 700 μL of $\text{DMSO}-d_6$ and the $^1\text{H NMR}$ spectrum recorded (Supporting Information Figure S2).

Chemical Detection of H_2S with Lead Acetate. To get qualitative chemical evidence for H_2S released in the presence of TCEP, we used the qualitative test for H_2S with lead acetate ($\text{Pb}(\text{OAc})_2$). H_2S reacts with Pb^{2+} to form PbS , which has a brownish to black color depending on the amount of H_2S . To a 1.5 mL Eppendorf tube with 1.0 mL of PBS (pH 7.4) containing 50 μM PEG–ADT was added TCEP (aq) to give a final concentration of 500 μM . Immediately, a Whatman paper impregnated with 100 μL of a 50 mM $\text{Pb}(\text{OAc})_2$ solution was

placed on top. Solutions containing ADT–OH and ADT– OCH_3 at 50 μM in 1% DMSO/PBS and without H_2S donor were reacted under the same conditions. After 1 h, H_2S release was confirmed by the formation of PbS on the filter paper. To confirm the absence of H_2S generation from ADT–OH in PBS, the reaction was repeated on a larger scale. A 15 mL Falcon tube was filled with 10 mL of a 50 μM solution in PBS containing ADT–OH or ADT– OCH_3 and reacted with or without TCEP at 500 μM final concentration. Upon mixing, the tubes were closed immediately so that any released H_2S could be directly trapped with a $\text{Pb}(\text{OAc})_2$ -impregnated filter paper inserted at the top and not in contact with the solution. After 1 week, H_2S release was confirmed by the formation of PbS on the filter paper.

Cell Culture. RAW-Blue macrophages were cultured in DMEM GlutaMAX supplemented with 10% heat-inactivated fetal bovine serum, 50 U/mL to 50 $\mu\text{g}/\text{mL}$ penicillin–streptomycin and 200 mg/mL Zeocin in a CO_2 incubator at 37 °C. Cells were passaged when reaching 70–80% confluency.

Preparation of Cell Lysate. RAW-Blue macrophages at 80% confluency were scraped off and centrifuged at 500 rpm for 5 min. The cell pellet was washed with cold Dulbecco's phosphate buffered saline (PBS) three times. The cell suspension was centrifuged at 500 rpm for 5 min, resuspended in passive lysis buffer at 1×10^7 cells/mL, and vortexed at RT for 10 min. The suspension was centrifuged, and the clear supernatant was collected and stored at –20 °C.

Measurement of H_2S Release in Cell Lysate by H_2S Electrode Sensor. Degassed PBS containing 10 vol % FBS or 20 vol % cell lysate (1 mL) was placed in a four-port closed chamber and incubated at 37 °C. After the sensor signal became stable, 50 μL of the PEG–ADT conjugate solutions was added (final concentration: 50 μM) using a Hamilton syringe. Released H_2S was recorded on a four-channel free radical analyzer.

Chemical Detection of H_2S with Dansylazide. To detect H_2S release qualitatively from cell lysate, dansylazide was used. The azide is reduced by H_2S and generates a fluorescent product that can be readily visualized with an UV lamp.⁴⁶ To validate this method, the experiment of H_2S detection from ADT– OCH_3 in the presence of TCEP was repeated with filter paper impregnated with 100 μL of saturated solution of dansylazide in 0.5% Tween/PBS pH 7.4. For detection of H_2S from ADT– OCH_3 and PEG–ADT in the presence of cell lysate, the following setup was used. A 2 mL glass HPLC vial with a stirring bar was filled with 670 μL (ADT– OCH_3) or 900 μL (PEG–ADT) of 20 vol % cell lysate/PBS pH 7.4 and 6.7 μL of ADT– OCH_3 in DMSO or 9.0 μL of PEG–ADT in H_2O was added (final concentration 50 μM). As control, 670 and 900 μL of 20 vol % cell lysate/PBS pH 7.4 solutions without donor were prepared. The Teflon seal of the sample vial was replaced with a filter paper impregnated with 25 μL of a saturated solution of dansylazide in 0.5% Tween/PBS pH 7.4. After attaching the screw cap, the vial was transferred to a larger vial and capped. The mixture was stirred for 24 h at RT. The filter papers were removed, put in small transparent plastic bags, and visualized with a Biorad Gel Doc EZ imager.

Measurement of H_2S Release in Cell Lysate by the Fluorescent Dye WSP-1. To a black well polystyrene plate containing 100 μL of 20 vol % cell lysate/PBS pH 7.4 were added 1 μL of ADT– OCH_3 in DMSO or 1 μL of PEG–ADT in H_2O (final concentration 50 μM) and 10 μL of WSP-1 in acetonitrile (final concentration 100 μM). As a control, cell

lysate without donor was measured as well. Immediately after adding, the fluorescence was measured on a Tecan well plate reader ($\lambda_{\text{ex}} = 465 \text{ nm}$, $\lambda_{\text{em}} = 515 \text{ nm}$).

Measurement of H_2S Concentration in Cell Culture Medium by the Fluorescent Dye WSP-1. RAW-Blue macrophages were seeded in a 96-well plate (5×10^4 cells/well) and cultured for 1 d. The medium was replaced with 100 μL /well of fresh medium and 1 μL /well of ADT-OH in DMSO, 5 μL /well of the PEG-ADT conjugate in water were added (final concentration of ADT: 100 μM). At different time points, 5 μL of medium was withdrawn and diluted with 45 μL of PBS. This sample solution was immediately mixed with 50 μL of WSP-1/DMSO (100 μM). A serial dilution of Na_2S in PBS was used as a standard. Fluorescence intensity ($\lambda_{\text{ex}} = 465 \text{ nm}$, $\lambda_{\text{em}} = 515 \text{ nm}$) was measured on a Tecan well plate reader.

Cell Viability Assay by the MTT Assay. RAW-Blue macrophages were seeded in a 96-well plate (1×10^5 cells/well) and cultured for 1 d. The medium was replaced with 100 μL /well of fresh medium and 1 μL /well of ADT-OH in DMSO and 5 μL /well of the PEG-ADT conjugate in LPS-free water with different concentrations were added. Cells were cultured for 1 d in a CO_2 incubator at 37 $^\circ\text{C}$. Thereafter, the medium was replaced with 100 μL /well fresh medium and 10 μL of MTT solution (5 mg/mL in PBS) was added to each well. The plate was incubated for 2 h at 37 $^\circ\text{C}$. Then, 100 μL of 0.1 g/mL sodium dodecyl sulfate in 0.01 M HCl (aq) was added to each well to lyse cells and solubilize formazan crystals. The OD at 570 nm was measured.

Live/Dead Assay. RAW-Blue macrophages were seeded in a triple-wells glass-based dish (5×10^4 cells/well) and cultured for 1 d. The medium was replaced with 200 μL /well of fresh medium containing 2 μL of ADT-OH in DMSO and 20 μL of the PEG-Gly-ADT, PEG-Ile-ADT, and PEG-ADT conjugates in LPS-free water were added (final concentration: 200 μM). After 1 d of culture, cells were washed with PBS and stained using the live/dead cell vitality assay kit according to the manufacturer's procedure. Cells were observed with an Olympus FluoView FV1000-D confocal microscope.

Observation of Intracellular Distribution of H_2S Donors. RAW-Blue macrophages were seeded in a triple-wells glass-based dish (5×10^4 cells/well) and cultured for 1 d. The medium was replaced with 200 μL /well of fresh medium containing 1 mg/mL rhodamine-labeled dextran (10 kDa) and 2 μL of FITC-labeled ADT-OH in DMSO (final concentration: 70 μM) and 20 μL of FITC-labeled PEG-ADT conjugate in water (final concentration: 100 μM) were added. After 4 h of culture, cells were washed with PBS and 100 μL /well of fresh medium was added. Cells were observed with an Olympus FluoView FV1000-D confocal microscope.

Lipopolysaccharide-Induced Inflammation. RAW-Blue cells were seeded at 5×10^4 cells/well in a 96-well plate and cultured for 1 d. The medium was replaced with 100 μL /well fresh medium containing 1 μL of ADT-OH in DMSO, 10 μL of Na_2S , and 10 μL of the PEG-ADT conjugate in LPS-free water were added (final concentration: 50 μM). Cells were stimulated with 1 $\mu\text{g}/\text{mL}$ LPS for 2 h, and the supernatant was analyzed by ELISA. Statistical analysis was performed using the Student *t* test.

Instrumentation. **NMR Spectroscopy.** ^1H NMR spectra were measured with a Bruker DPX400 NMR spectrometer. A total of 32 scans were collected, and the D1 was set to 10 s. Chemical shifts are referenced to residual undeuterated NMR solvent signal at 2.50 ppm ($\text{DMSO}-d_6$) and 7.26 ppm (CDCl_3).

UV/Vis Spectroscopy. Absorbance and spectra were measured on a Tecan infinite M200 in transparent polystyrene 96-well plates.

H_2S Electrode Sensor. H_2S was measured by monitoring the change in current in pA with a World Precision Instruments ISO-H2S-2 hydrogen sulfide sensor coupled to a four-channel free radical analyzer. The measurement chamber was kept at 37 $^\circ\text{C}$ using a thermostatic bath, and the temperature was measured with a temperature sensor.

High Resolution Mass Spectrometry. ESI-TOF MS analyses were performed on a Bruker microTOFII mass spectrometer.

Confocal Laser Scanning Fluorescence Microscopy (CLSM). Fluorescent images were acquired on an Olympus FluoView FV1000-D confocal microscope equipped with 405, 473, 559, and 635 nm lasers.

■ ASSOCIATED CONTENT

§ Supporting Information

UV/vis spectra of PEG-Gly-ADT, PEG-ADT, and ADT-OH, ^1H NMR spectra of hydrolysis PEG-Gly-ADT, and PEG-Ile-ADT in cell culture, qualitative detection of H_2S by lead acetate and dansylazide, structure of WSP-1, synthesis of FITC-labeled ADT-OH and PEG-ADT conjugate. This material is available free of charge via the Internet at <http://pubs.acs.org>.

■ AUTHOR INFORMATION

Corresponding Author

*Phone: +81-6-6879-7365. Fax: +81-6-6879-7367. E-mail: urara.hasegawa@chem.eng.osaka-u.ac.jp. Address: 2-1, Yamadaoka, Suita, Osaka 565-0871, Japan.

Notes

The authors declare no competing financial interest.

■ ACKNOWLEDGMENTS

We thank Prof. Hiroshi Uyama as well as Prof. Takashi Hayashi and Prof. Koji Oohora (Osaka University, Japan) for ESI-TOF MS analysis. This work was supported by Grant-in-Aid for Young Scientists (B), no. 24700482, from the Japan Society for the Promotion of Science.

■ REFERENCES

- (1) Wang, R. (2002) Two's company, three's a crowd: can H_2S be the third endogenous gaseous transmitter? *FASEB J.* 16, 1792–1798.
- (2) Beauchamp, R., Bus, J., Popp, J., Boreiko, C., and Andjelkovich, D. (1984) A critical review of the literature on hydrogen sulfide toxicity. *Crit. Rev.Toxicol.* 13, 25–97.
- (3) Reiffenstein, R., Hulbert, W., and Roth, S. (1992) Toxicology of hydrogen sulfide. *Annu. Rev. Pharmacol. Toxicol.* 32, 109–134.
- (4) Qu, K., Lee, S. W., Bian, J. S., Low, C. M., and Wong, P. T. H. (2008) Hydrogen sulfide: neurochemistry and neurobiology. *Neurochem. Int.* 52, 155–165.
- (5) Caliendo, G., Cirino, G., Santagada, V., and Wallace, J. L. (2010) Synthesis and biological effects of hydrogen sulfide (H_2S): Development of H_2S -releasing drugs as pharmaceuticals. *J. Med. Chem.* 53, 6275–6286.
- (6) Ida, T., Sawa, T., Ihara, H., Tsuchiya, Y., Watanabe, Y., Kumagai, Y., Suematsu, M., Motohashi, H., Fujii, S., Matsunaga, T., Yamamoto, M., Ono, K., Devarie-Baez, N. O., Xian, M., Fukuto, J. M., and Akaike, T. (2014) Reactive cysteine persulfides and S-polythiolation regulate oxidative stress and redox signaling. *Proc. Natl. Acad. Sci. U.S.A.* 111, 7606–7611.
- (7) Kimura, H. (2014) The physiological role of hydrogen sulfide and beyond, *Nitric Oxide*, doi: 10.1016/j.niox.2014.01.002.

- (8) Wagner, F., Asfar, P., Calzia, E., Radermacher, P., and Szabo, C. (2009) Bench-to-bedside review: hydrogen sulfide, the third gaseous transmitter: applications for critical care. *Crit. Care* 13, 213.
- (9) Szabo, C. (2007) Hydrogen sulphide and its therapeutic potential. *Nature Rev. Drug Discovery* 6, 917–935.
- (10) Olson, K. R. (2011) The therapeutic potential of hydrogen sulfide: separating hype from hope. *Am. J. Physiol.: Regul., Integr. Comp. Physiol.* 301, R297–R312.
- (11) Greiner, R., Pálkás, Z., Bäsell, K., Becher, D., Antelmann, H., Nagy, P., and P, D. T. (2013) Polysulfides link H₂S to protein thiol oxidation. *Antioxid. Redox. Signal.* 19, 1749–1765.
- (12) Li, L., Whiteman, M., Guan, Y. Y., Neo, K. L., Cheng, Y., Lee, S. W., Zhao, Y., Baskar, R., Tan, C.-H., and Moore, P. K. (2008) Characterization of a novel, water-soluble hydrogen sulfide-releasing molecule (GY4137): new insights into the biology of hydrogen sulfide. *Circulation* 117, 2351–2360.
- (13) Long, M. J. D., Dolan, P., Santamaria, A. B., and Bueding, E. (1986) 1, 2-Dithiol-3-thione analogs: effects on NAD(P)H: quinone reductase and glutathione levels in murine hepatoma cells. *Carcinogenesis* 7, 977–980.
- (14) Zhang, Y., and Munday, R. (2008) Dithiolethiones for cancer chemoprevention: where do we stand? *Mol. Cancer Ther.* 7, 3470–3479.
- (15) Nagano, T., and Takeyama, M. (2001) Enhancement of salivary secretion and neuropeptide (substance P, α -calcitonin gene-related peptide) levels in saliva by chronic anethole trithione treatment. *J. Pharm. Pharmacol.* 53, 1697–1702.
- (16) Lam, S., MacAulay, C., le Riche, J. C., Dyachkova, Y., Coldman, A., Guillaud, M., Hawk, E., Christen, M.-O., and Gazdar, A. F. (2002) A randomized phase IIb trial of anethole dithiolethione in smokers with bronchial dysplasia. *J. Natl. Cancer Inst.* 94, 1001–1009.
- (17) Reddy, B. S., Rao, C. V., Rivenson, A., and Kelloff, G. (1993) Chemoprevention of colon carcinogenesis by organosulfur compounds. *Cancer Res.* 53, 3493–3498.
- (18) Lubet, R. A., Steele, V. E., Eto, I., Juliana, M. M., Kelloff, G. J., and Grubbs, C. J. (1997) Chemopreventive efficacy of anethole trithione, N-acetyl-L-cysteine, miconazole and phenethylisothiocyanate in the DMBA-induced rat mammary cancer model. *Int. J. Cancer* 72, 95–101.
- (19) Drukarch, B., Schepens, E., Stoof, J. C., and Langeveld, C. H. (1997) Anethole dithiolethione prevents oxidative damage in glutathione-depleted astrocytes. *Eur. J. Pharmacol.* 329, 259–262.
- (20) Mansuy, D., Sassi, A., Dansette, P. M., and Plat, M. (1986) A new potent inhibitor of lipid peroxidation in vitro and in vivo, the hepatoprotective drug anisylthiothione. *Biochem. Biophys. Res. Commun.* 135, 1015–1021.
- (21) Warnet, J. M., Christen, M. O., Thevenin, M., Biard, D., Jacqueson, A., and Claude, J. R. (1989) Protective effect of anethol dithiothione against acetaminophen hepatotoxicity in mice. *Pharmacol. Toxicol.* 65, 63–64.
- (22) Chen, P., Luo, Y., Hai, L., Qian, S., and Wu, Y. (2010) Design, synthesis, and pharmacological evaluation of the aqueous prodrugs of desmethyl anethole trithione with hepatoprotective activity. *Eur. J. Med. Chem.* 45, 3005–3010.
- (23) Sen, C. K., Traber, K. E., and Packer, L. (1996) Inhibition of NF- κ B activation in human T-cell lines by anetholdithiothione. *Biochem. Biophys. Res. Commun.* 218, 148–153.
- (24) Switzer, C. H., Cheng, R. Y.-S., Ridnour, L. A., Murray, M. C., Tazzari, V., Sparatore, A., Del Soldato, P., Hines, H. B., Glynn, S. A., Ambs, S., and Wink, D. A. (2012) Dithiolethiones inhibit NF- κ B activity via covalent modification in human estrogen receptor-negative breast cancer. *Cancer Res.* 72, 2394–2404.
- (25) Sen, N., Paul, B. D., Gadalla, M. M., Mustafa, A. K., Sen, T., Xu, R., Kim, S., and Snyder, S. H. (2012) Hydrogen sulfide-linked sulfhydration of NF- κ B mediates its antiapoptotic actions. *Mol. Cell* 45, 13–24.
- (26) Duncan, R. (2003) The dawning era of polymer therapeutics. *Nature Rev. Drug Discovery* 2, 347–360.
- (27) Ringsdorf, H. (1975) Structure and properties of pharmacologically active polymers. *J. Polym. Sci., Polym. Symp.* 51, 135–153.
- (28) Maeda, H. (2001) The enhanced permeability and retention (EPR) effect in tumor vasculature: the key role of tumor-selective macromolecular drug targeting. *Adv. Enzyme Regul.* 41, 189–207.
- (29) Kashfi, K., and Olson, K. R. (2013) Biology and therapeutic potential of hydrogen sulfide and hydrogen sulfide-releasing chimeras. *Biochem. Pharmacol.* 85, 689–703.
- (30) Whiteman, M., and Winyard, P. G. (2011) Hydrogen sulfide and inflammation: the good, the bad, the ugly and the promising. *Expert Rev. Clin. Pharmacol.* 4, 13–32.
- (31) Fiorucci, S., Distrutti, E., Cirino, G., and Wallace, J. L. (2006) The emerging roles of hydrogen sulfide in the gastrointestinal tract and liver. *Gastroenterology* 131, 259–271.
- (32) Fiorucci, S., Orlandi, S., Mencarelli, A., Caliendo, G., Santagada, V., Distrutti, E., Santucci, L., Cirino, G., and Wallace, J. L. (2007) Enhanced activity of a hydrogen sulphide-releasing derivative of mesalamine (ATB-429) in a mouse model of colitis. *Br. J. Pharmacol.* 150, 996–1002.
- (33) Sparatore, A., Perrino, E., Tazzari, V., Giustarini, D., Rossi, R., Rossoni, G., Erdman, K., Schröder, H., and Soldato, P. D. (2009) Pharmacological profile of a novel H₂S-releasing aspirin. *Free Radical Biol. Med.* 46, 586–592.
- (34) Li, L., Rossoni, G., Sparatore, A., Lee, L. C., Del Soldato, P., and Moore, P. K. (2007) Anti-inflammatory and gastrointestinal effects of a novel diclofenac derivative. *Free Radical Biol. Med.* 42, 706–719.
- (35) Wallace, J. L., Caliendo, G., Santagada, V., and Cirino, G. (2010) Markedly reduced toxicity of a hydrogen sulphide-releasing derivative of naproxen (ATB-346). *Br. J. Pharmacol.* 159, 1236–1246.
- (36) Distrutti, E., Sediari, L., Mencarelli, A., Renga, B., Orlandi, S., Russo, G., Caliendo, G., Santagada, V., Cirino, G., Wallace, J. L., and Fiorucci, S. (2006) 5-Amino-2-hydroxybenzoic acid 4-(S-thioxo-5H-[1,2]dithiol-3yl)-phenyl ester (ATB-429), a hydrogen sulfide-releasing derivative of mesalamine, exerts antinociceptive effects in a model of postinflammatory hypersensitivity. *J. Pharmacol. Exp. Ther.* 319, 447–458.
- (37) Perrino, E., Cappelletti, G., Tazzari, V., Giavini, E., Soldato, P. D., and Sparatore, A. (2008) New sulfurated derivatives of valproic acid with enhanced histone deacetylase inhibitory activity. *Bioorg. Med. Chem. Lett.* 18, 1893–1897.
- (38) Tazzari, V., Cappelletti, G., Casagrande, M., Perrino, E., Renzi, L., Del Soldato, P., and Sparatore, A. (2010) New aryl dithiolethione derivatives as potent histone deacetylase inhibitors. *Bioorg. Med. Chem.* 18, 4187–4194.
- (39) Benavides, G. A., Squadrito, G. L., Mills, R. W., Patel, H. D., Isbell, T. S., Patel, R. P., Darley-Usmar, V. M., Doeller, J. E., and Kraus, D. W. (2007) Hydrogen sulfide mediates the vasoactivity of garlic. *Proc. Natl. Acad. Sci. U. S. A.* 104, 17977–17982.
- (40) Zhao, Y., Wang, H., and Xian, M. (2010) Cysteine-activated hydrogen sulfide (H₂S) donors. *J. Am. Chem. Soc.* 133, 15–17.
- (41) Zanatta, S. D., Jarrott, B., and Williams, S. J. (2010) Synthesis and preliminary pharmacological evaluation of aryl dithiolethiones with cyclooxygenase-2-selective inhibitory activity and hydrogen sulfide-releasing properties. *Aust. J. Chem.* 63, 946–957.
- (42) Lee, M., Tazzari, V., Giustarini, D., Rossi, R., Sparatore, A., Del Soldato, P., McGeer, E., and McGeer, P. L. (2010) Effects of hydrogen sulfide-releasing L-DOPA derivatives on glial activation: potential for treating parkinson disease. *J. Biol. Chem.* 285, 17318–17328.
- (43) Sugii, A., Kabasawa, Y., and Akamatsu, T. (1968) Polarographic studies on pharmaceuticals. II: Polarography of the anethole trithione. *J. Pharm. Soc. Jpn.* 88, 1371–1374.
- (44) Yu, F., Li, P., Song, P., Wang, B., Zhao, J., and Han, K. (2012) An ICT-based strategy to a colorimetric and ratiometric fluorescence probe for hydrogen sulfide in living cells. *Chem. Commun.* 48, 2852–2854.
- (45) Liu, C., Pan, J., Li, S., Zhao, Y., Wu, L. Y., Berkman, C. E., Whorton, A. R., and Xian, M. (2011) Capture and visualization of hydrogen sulfide by a fluorescent probe. *Angew. Chem., Int. Ed.* 50, 10327–10329.

(46) Peng, H., Cheng, Y., Dai, C., King, A. L., Predmore, B. L., Lefer, D. J., and Wang, B. (2011) A fluorescent probe for fast and quantitative detection of hydrogen sulfide in blood. *Angew. Chem., Int. Ed.* 50, 9672–9675.

(47) Luxenhofer, R., Sahay, G., Schulz, A., Alakhova, D., Bronich, T. K., Jordan, R., and Kabanov, A. V. (2011) Structure–property relationship in cytotoxicity and cell uptake of poly(2-oxazoline) amphiphiles. *J. Controlled Release* 153, 73–82.

(48) Conner, S. D., and Schmid, S. L. (2003) Regulated portals of entry into the cell. *Nature* 422, 37–44.

(49) Scholz, M., Ulbrich, H. K., Soehnlein, O., Lindbom, L., Mattern, A., and Dannhardt, G. (2009) Diaryl-dithiolanes and -isothiazoles: COX-1/COX-2 and 5-LOX-inhibitory, OH scavenging and anti-adhesive activities. *Bioorg. Med. Chem.* 17, 558–568.

(50) van der Vlies, A. J., Hasegawa, U., and Hubbell, J. A. (2012) Reduction-sensitive tioguanine prodrug micelles. *Mol. Pharmaceutics* 9, 2812–2818.